Title

Shp2 deletion in hepatocytes suppresses hepatocarcinogenesis driven by oncogenic β-Catenin, PIK3CA and MET

Journal

Journal of Hepatology, 69(1)

ISSN

0168-8278

Authors

Liu, Jacey J
Li, Yanjie
Chen, Wendy S
et al.

Publication Date

2018-07-01

DOI

10.1016/j.jhep.2018.02.014

Peer reviewed

HHS Public Access

Author manuscript

J Hepatol. Author manuscript; available in PMC 2019 July 01.

Published in final edited form as:

J Hepatol. 2018 July ; 69(1): 79–88. doi:10.1016/j.jhep.2018.02.014.

Shp2 Deletion in Hepatocytes Suppresses Hepatocarcinogenesis Driven by Oncogenic β-Catenin, PIK3CA and MET

Jacey J. Liu[1,#], **Yanjie Li**[1,2,#], **Wendy S. Chen**[1], **Yan Liang**[1], **Gaowei Wang**[1], **Min Zong**[1], **Kota Kaneko**[1], **Ruiyun Xu**[2], **Michael Karin**[3], and **Gen-Sheng Feng**[1,*]

[1]Department of Pathology, and Division of Biological Sciences, Moores UCSD Cancer Center, University of California San Diego, La Jolla, CA, USA

[2]Department of Hepatobiliary Surgery, 3rd affiliated Hospital, Sun Yat-sen University, Guangzhou, China

[3]Departments of Pharmacology and Pathology, University of California San Diego, La Jolla, CA, USA

Abstract

Background and Aims—Shp2 is an SH2-tyrosine phosphatase acting downstream of receptor tyrosine kinases (RTKs). Most recent data demonstrated a liver tumor-suppressing role for Shp2, as ablating Shp2 in hepatocytes aggravated hepatocellular carcinoma (HCC) induced by chemical carcinogen or Pten loss. We further investigated the effect of Shp2 deficiency on liver tumorigenesis driven by classical oncoproteins c-Met (receptor for HGF), β-catenin and PIK3CA.

Methods—We performed hydrodynamic tail vein injection of two pairs of plasmids expressing c-Met and ΔN90-β-catenin (MET/CAT), or c-Met and PIK3CA^{H1047R} (MET/PIK), into *WT* and *Shp2*$^{hep-/-}$ mice. We compared liver tumor loads, and investigated the pathogenesis and molecular mechanisms using multidisciplinary approaches.

Results—Despite the induction of oxidative and metabolic stresses, Shp2 deletion in hepatocytes suppressed hepatocarcinogenesis driven by overexpression of oncoproteins MET/CAT or MET/PIK. Shp2 loss inhibited proliferative signaling from c-Met, Wnt/β-catenin, Ras/Erk and PI3K/Akt pathways, but triggered cell senescence following exogenous expression of the oncogenes.

Corresponding author: Gen-Sheng Feng, Mail address: Mail code 0864, University of California San Diego, 9500 Gilman Drive, La Jolla, CA 92093; Phone: 858-822-5441; gfeng@ucsd.edu.
[#]J.J. Liu and Y. Li made equal contributions to the work.

Conflict of interest: The authors have no conflict of interest to disclose.

Authors' contributions: Jacey Liu, Yanjie Li, Wendy Chen, Min Zong and Kota Kaneko were involved in data acquisition and analysis. Yan Liang and Gaowei Wang were involved in RNA-seq data analysis and interpretation. Ruiyun Xu was involved in supervision of Yanjie Li's experiment, Michael Karin provided the *Ikkβ*$^{fl/fl}$ mouse line and data analysis. Jacey Liu, Wendy Chen and Yan Liang were involved in the manuscript writing. Gen-Sheng Feng was involved in study concept and design, interpretation of data, drafting and critical revision of manuscript. Jacey J. Liu and Yanjie Li made equal contributions to the manuscript as co-first authors. Gen-Sheng Feng is the corresponding author. All Authors have seen and approved the manuscript being submitted.

Conclusions—Shp2, acting downstream of RTKs, is positively required for hepatocyte-intrinsic tumorigenic signaling from these oncoproteins, even if Shp2 deficiency induces a tumor-promoting hepatic microenvironment. These data suggest a new and more effective therapeutic strategy for HCCs driven by oncogenic RTKs and other upstream molecules, by inhibiting Shp2 and also suppressing any tumor-enhancing stromal factors produced due to Shp2 inhibition.

Lay Summary—Primary liver cancer is a most malignant disease with no effective therapeutic means available. We show here that a cytoplasmic tyrosine phosphatase Shp2 is required for liver tumorigenesis driven by two oncoproteins that are implicated in human liver cancer. This, together with our previous studies, uncovers the complexity in mechanisms of liver tumorigenesis, by deciphering the pro- and anti-tumor effects of Shp2 in mouse models.

Graphical abstract

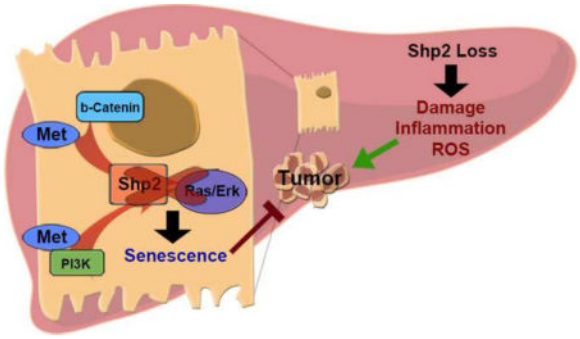

Keywords

Liver tumorigenesis; Shp2; Met; β-catenin; PIK3CA

Introduction

Primary liver cancer, mainly hepatocellular carcinoma (HCC), is a most malignant disease worldwide. While the overall cancer mortality and incidences are decreasing, liver cancer incidences are increasing rapidly in the United States[1]. The lack of effective therapeutic drug is evidently due to poor understanding of the complicated mechanisms of hepatocarcinogenesis.

Ptpn11 encodes a cytoplasmic tyrosine phosphatase Shp2 that can dock directly on ligand-activated receptor tyrosine kinases (RTKs) through its two SH2 domains[2], which immediately implicated a putative role of Shp2 in dephosphorylation and inactivation of RTKs. However, genetic and biochemical data have disclosed a positive effect of this phosphatase in augmenting cytoplasmic signaling through the Erk pathway, proximal to RTKs[2,3]. Consistently, *Ptpn11/Shp2* has been identified as the first proto-oncogene that encodes a tyrosine phosphatase, with dominant active mutations detected in leukemia patients with or without Noonan Syndrome[4,5]. In contrast, our most recent experiments demonstrated a tumor-inhibitory role for Shp2 in liver cancer, because ablating Shp2 in hepatocytes triggered hepatocellular adenoma (HCA) in aged mice and also enhanced HCC development induced by diethylnitrosamine (DEN)[6]. Simultaneous deletion of Shp2 and

Pten in hepatocytes dramatically accelerated and enhanced non-alcoholic steatohepatitis (NASH) and liver tumorigenesis[7], indicating concerted tumor-inhibitory activities of Shp2 and Pten in guarding hepatic homeostasis and functions. Consistent with the animal data, concomitant Pten and Shp2 deficiencies were detected in HCC patients with poor prognosis[7]. These results indicate an anti-oncogenic role of Shp2 in the liver, in contrast to its pro-leukemogenic effect in the hematopoietic system. Similarly, several other groups reported that deleting some classical oncoproteins, such as c-MET, EGFR, β-catenin, Ikkβ and Jnk1/2 and Akt1/2, ironically exacerbated DEN-induced HCC development, although the underlying mechanisms are not fully understood[8–10].

To further dissect Shp2 functions in liver cancer, we examined the effect of Shp2 deficiency in mouse tumor models induced by c-MET and an oncogenic β-catenin mutant (MET/CAT). Co-activation of MET and β-catenin signaling has been detected in human HCC patients[11], and hydrodynamic tail vein injection of MET/CAT oncogenes has been shown to efficiently induce HCC development in mice[11–13]. Surprisingly, Shp2 removal in hepatocytes suppressed HCC driven by MET/CAT injection, in spite of the hepatic inflammation and fibrosis, and increased oxidative stress in Shp2-deficient liver. Shp2 deletion also inhibited liver tumorigenesis driven by co-expression of c-MET and PIK3CA (MET/PIK), suggesting a requirement of Shp2 in relay of these oncogenic signals in the liver.

Materials and Methods

Experimental mice

The *Shp2*$^{hep-/-}$ (*Shp2*$^{fl/fl}$*:Alb-Cre*$^{+}$) mouse line in C57BL/6 background was generated by breeding *Shp2*$^{fl/fl}$ mouse with *Albumin-Cre* transgenic mice, as previously described[6,14]. All animal studies were conducted on male *Shp2*$^{fl/fl}$ (*WT*) or *Shp2*$^{fl/fl}$*:Alb-Cre(Shp2*$^{hep-/-}$*)* mice at age of 6–23 weeks. Mice were group-housed (2–5 mice per cage) expect for less than 5% of mice were single-housed in later time period due to death of cage-mates. All mice were maintained under a 12 h light/dark cycle with free access to water and standard mouse chow. The animal protocols (S09108) and all of the experimental procedures were approved by the Institutional Animal Care and Use Committee (IACUC) of the University of California San Diego. For Hydrodynamic injection, plasmids (*met*: PT3EF1aH-hMet; *ctnnb1/β-catenin*: PT3EF1aH-*β*-catenin; *pik3ca*: PIK3CA-H1047RΔf-PT3EF5a; *sleeping beauty transposase(SB)*: pCMV/SB) were kindly provided by Dr. X. Chen at UCSF. Oncogene-expressing constructs were delivered by hydrodynamic tail vein injection into mice at 6–8 weeks of age, as described previously[12].

Statistical analysis

For RNA-seq analysis, significant differences in gene expression were identified by FDR<0.05, and enriched pathways or gene sets were identified by P<0.05 or FDR-q<0.05. For other studies, statistical analysis was done using GraphPad Prism 7. Statistical significance between means was calculated by student's t test. P value <0.05 was considered significant (*P<0.05; **P<0.01; ***P<0.001).

Results

Shp2 is required for MET/β-catenin-driven hepatocarcinogenesis

In previous experiments, we generated a mutant mouse line with hepatocyte-specific Shp2 deletion (*Shp2*$^{hep-/-}$)[14]. Shp2 deficiency, while impairing hepatocyte proliferation following partial hepatectomy[14], also triggered HCA development in old mice and exacerbated DEN-induced HCC[6]. In this study, we induced liver tumorigenesis in *WT* control and *Shp2*$^{hep-/-}$ mice, following hydrodynamic tail vein injection of two plasmids that express human MET (hMET) and a truncated β-catenin mutant, ΔN90-β-catenin (MET/CAT), together with the SB transposase[13,15]. By examining the liver phenotype at different time points, we detected multiple tumor nodules in control mice 8 weeks after injection of the oncogenes (Fig. 1A). However, Shp2 deficiency in hepatocytes resulted in marked reduction of tumor burdens induced by MET/CAT, as evaluated by the liver versus body weight ratios, tumor incidences, and the maximal sizes of tumor lesions (Fig. 1B). Histological analysis indicated that the tumors were mainly HCC (Fig. 1A, and Supplementary Fig. 1). Thus, removing Shp2 in hepatocytes efficiently suppressed MET/CAT-driven liver tumorigenesis, in sharp contrast to the previous data showing that Shp2 deficiency dramatically aggravated DEN-induced HCC development in the same *Shp2*$^{hep-/-}$ mouse line[6]. We examined the pathogenic process following oncogene injection, and found that tumor nodules were visible in *WT* mice by 5 weeks and progressed rapidly at 8 weeks (Fig. 1A). Tumor nodules were barely detectable in oncogene-injected *Shp2*$^{hep-/-}$ livers, with some lesions observed, including scalloped edges and slightly lumpy surface, as described previously[6].

Shp2 is also necessary for MET/PIK3CA-induced liver tumorigenesis

We then examined the effect of Shp2 loss on liver tumorigenesis driven by another pair of oncogenes, hMET and PIK3CA^{H1047R} (MET/PIK). PIK3CA represents dominant active mutants of the p110α catalytic subunit of phosphatidylinositol-3-kinase (PI3K), which have been detected in several types of cancer[16]. Chen and colleagues demonstrated[17] that hydrodynamic delivery of PIK3CA alone induced hepatic steatosis but not tumorigenesis, while co-transfection of PIK3CA with hMET or NRasV12 robustly induced liver tumor. Consistently, we detected liver tumors in *WT* mice at 12 weeks after injection of MET/PIK (Fig. 2A). Unlike the MET/CAT combination that induced tumor nodules clearly visible on liver surface, MET/PIK triggered non-alcoholic fatty liver disease (NAFLD) and diffused tumors in the liver. At 6 weeks following MET/PIK transfection, the *WT* mice developed NAFLD and progressed rapidly, with tumors first detected around 9 weeks post injection. The *Shp2*$^{hep-/-}$ mice exhibited significantly decreased susceptibility to MET/PIK-driven liver tumorigenesis, as evaluated by the ratio of liver to body weights and pathological analysis (Fig. 2A–B). Shp2 deletion also caused the liver less susceptible to MET/PIK-induced NAFLD, as revealed by less lipid accumulation during the time period and Oil-red-O staining of liver sections (Fig. 2A,C). When examined at 15 weeks, we did observe a few tumor nodules in some *Shp2*$^{hep-/-}$ livers (Supplementary Fig. 2A). However, immunoblotting detected Shp2 protein in the tumor tissues, with the surrounding hepatic tissues being Shp2-negative (Supplementary Fig. 2B). Thus, the tumors were likely grown from hepatocytes that escaped Cre-mediated *Shp2/Ptpn11* deletion in *Shp2*$^{hep-/-}$ livers,

reinforcing the requirement of Shp2 for MET/PIK-driven liver tumorigenesis. Similarly, a previous report showed presence of β-catenin in tumor cells in *ctnnb1*$^{hep-/-}$ livers[18].

We then asked if Ikkβ a kinase that activates NF-κB pathway, is also required for MET/CAT- or MET/PIK-driven liver cancer. Like Shp2 loss, deleting Ikkβ was shown to exacerbate DEN-induced HCC development[19,20], although a positive role of NF-κB signaling in driving HCC was also reported[21]. Similar tumor burdens were detected in *WT* control and *Ikkβ*$^{hep-/-}$ mice, examined at 8 or 12 weeks after transfection of MET/CAT and MET/PIK, respectively (Supplementary Fig. 3A–C). As revealed by Oil-Red-O staining, Ikkβ loss did not have a significant impact on NAFLD induced by MET/PIK (Supplementary Fig. 3B). Therefore, despite similar aggravating effects of Ikkβ and Shp2 deficiencies on DEN-induced HCC[6,19], Ikkβ loss in hepatocytes did not have significant impact on liver tumorigenesis driven by either MET/CAT or MET/PIK. Together, these results define a specific requirement of endogenous Shp2 in liver tumorigenesis at least driven by these two pairs of oncogenes.

Shp2$^{hep-/-}$ liver is characterized by impaired proliferative capacity and increased oxidative and metabolic stresses

To explore the mechanism underlying the unique Shp2 function, we conducted RNA-seq analysis to compare the transcriptomes in *WT* and *Shp2*$^{hep-/-}$ livers, at day 0, 3 and 7 after delivery of MET/CAT or MET/PIK oncogenes. Overall, deleting Shp2 in hepatocytes caused dramatic changes in hepatic gene expression, before and after transfection of the oncogenes (Fig. 3A). We first analyzed the baseline transcriptomes in *WT* and *Shp2*$^{hep-/-}$ livers at day 0, to understand why Shp2 loss makes hepatocytes unsusceptible to the oncogenic effect of these potent oncoproteins. GSEA analysis showed that the cluster 1 highly expressed in *WT* livers was enriched for gene sets in mRNA transcription and processing (Fig. 3B), including *Srsf7, Hnrnpa2b1, Tra2b, Fus* and *Rbmx*, with *Srsf7, Tra2b* and *Hnrnpa2b1* identified as Myc targets[22]. The expression of these genes required for cell proliferation was in general decreased in *Shp2*$^{hep-/-}$ livers (Supplementary Fig. 4A–B), consistent with the previous data that Shp2 removal suppressed hepatocyte proliferation[14]. In particular, the expression of *pik3ri, jun*, and *fos*, genes downstream of the HGF/c-Met pathway, was downregulated in Shp2-deficient livers (Fig. 3C). Shp2 ablation also caused changes in expression of genes in the Wnt/β-catenin pathway, and most of the genes predicted to be upregulated by Wnt signaling expressed at higher levels in *WT* than *Shp2*$^{hep-/-}$ livers (Fig. 3D). Together, these results suggest a negative impact of Shp2 loss on the basal levels of signaling through the HGF/c-Met and Wnt/β-catenin pathways in the liver.

Relative to the *WT* control, the genes in cluster 2 highly expressed in *Shp2*$^{hep-/-}$ livers were featured by increased oxidative stress and reprogramming of metabolic pathways (Fig. 3B, Supplementary file 2). In particular, the highly expressed genes included *nsdhl, dhcr24, hsd17b7* and *cyp51a1* in cholesterol metabolism, *mgst1, gstk1* and *gpx1* in response to oxidative stress, and the PPARα pathway that regulates lipid metabolism (Fig. 3B, Supplementary file 2). Also highly expressed in Shp2-deficient livers were genes of nuclear receptor heterodimers PXR/RXR, LXR/RXR and FXR/RXR involved in modulation of metabolic processes (Fig. 3E). Together, the RNA-seq data suggest that Shp2 deletion

caused downregulation of hepatocyte proliferation potential, reprogramming of metabolic pathways and increased oxidative stress in the liver, before oncogene transfection.

Shp2 deletion disturbed multiple signaling events induced by MET/CAT or MET/PIK

The cluster 3 in MET/CAT-transfected *WT* livers did not provide much information except some genes involved in coagulation system and metabolism, such as *F11, PLG, LIPC* and *OTC* (Fig. 3B, Supplementary file 3). We then used IPA to compare the day 0 and 3 transcriptomes in *WT* and $Shp2^{hep-/-}$ livers separately (Fig. 4A). MET/CAT transfection triggered DNA damage response, coagulation, and fibrotic processes in both genotypes, in particular the z-score of G2/M checkpoint regulation calculated by IPA was lower in the *WT* liver (*WT*: −2; $Shp2^{hep-/-}$: −1.667). Genes related to the checkpoint control and cell cycle progression, such as *Plk1, Cdc25, Top2a, Cyclin B1* and *Cyclin B2*, were more abundantly expressed in the *WT* than the mutant livers, suggesting that Shp2 deletion affected the checkpoint passing and entry into M phase[23]. In contrast, upregulation of checkpoint regulators, including *p21* and *Brca1*, in $Shp2^{hep-/-}$ livers further suggests defective entry into M phase[24,25]. This point was reinforced by upregulation of p53 signaling (Fig. 4A) and positive regulation of p53 target genes (Supplementary Fig. 4E). Thus, although MET/CAT injection promoted cell proliferation in both genotypes, Shp2 deficiency led to suppression of cell cycle progression. In addition, we observed more severe inflammatory and immune responses in MET/CAT-transfected $Shp2^{hep-/-}$ livers, such as IL-10 signaling and dendritic cell maturation (Fig. 4A). Next, we compared the transcriptomes between *WT* and $Shp2^{hep-/-}$ livers at day 3 after MET/CAT transfection, and identified enrichment of gene sets in inflammatory response, leukocyte recruitment and cytokine secretion in $Shp2^{hep-/-}$ livers (Supplementary file 5). Of note, the downstream targets in NF-κB pathway was upregulated in $Shp2^{hep-/-}$ liver (Fig. 4D), accompanied by downregulation of Myc targets (Fig. 4E, Supplementary file 6). Impaired signaling to Myc pathway is likely one mechanism for inhibition of tumorigenesis in MET/CAT-transfected $Shp2^{hep-/-}$ liver.

The cluster 4 in MET/PIK-transfected *WT* livers at day 3 included genes in DNA replication and G2/M transition pathways, such as Aurora B and PLK1 (Fig. 3B). We then compared the day 0 and 3 transcriptomes in *WT* and $Shp2^{hep-/-}$ livers separately, using GSEA and IPA. MET/PIK injection triggered higher enrichment of several cell cycle-related pathways in *WT* livers (Fig. 4B), consistent with the identification of cluster 4 (Fig. 3B). In contrast, p53 signaling and cell cycle inhibitors such as Gadd45g and p21, were upregulated by MET/PIK in $Shp2^{hep-/-}$ livers (Fig. 4C), suggesting relative cell cycle suppression by Shp2 loss. MET/PIK injection also induced immune response in the liver of both genotypes (Fig. 4C; Supplementary file 11,12), likely due to stress response to oncogene overexpression. In comparison of the day 3 transcriptomes between $Shp2^{hep-/-}$ and *WT* livers, we found that Shp2 deletion caused increase in fatty acid metabolism and oxidative stress in response to MET/PIK (Fig. 4F, Supplementary file 7), consistent with the oxidative stress observed even in untreated $Shp2^{hep-/-}$ livers.

We further analyzed the gene expression profiles 7 days after oncogenes' delivery. A GFP-expressing plasmid was also injected into *WT* and $Shp2^{hep-/-}$ livers as vector control, and the transcriptomes after the vector injection were very similar to the day-0 untreated livers in

both genotypes (Supplementary Fig. 4D). The transcriptomes were very similar at day 3 and 7 in *WT* or *Shp2*$^{hep-/-}$ livers injected with the same oncogenes, but the differences in gene expression between the two genotypes remained very significant at day 7 after injection of the vector, MET/CAT or MET/PIK. Commonly enriched in untreated and vector-injected *Shp2*$^{hep-/-}$ livers were genes involved in redox reaction, metabolic and apoptosis pathways (Fig. 3F). Genes upregulated in MET/CAT-injected *WT* livers at day 7 were enriched in RNA transcription related genes and genes transcriptionally targeted by NF1 (Neurofibromin 1), a negative regulator of Ras (Fig. 4G). Enriched in MET/CAT-injected *Shp2*$^{hep-/-}$ livers were genes in immune response pathways and targets of GABPA (GA binding protein transcription factor, alpha subunit) (Fig. 4G). MET/PIK transfection induced cell cycle progression related pathways in *WT* liver, while *Shp2*$^{hep-/-}$ liver was featured by elevated immune response (Fig. 4H). The target genes of Myc and SP1 were downregulated in MET/PIK-injected *Shp2*$^{hep-/-}$ livers (Fig. 4H), suggesting impaired cell proliferation in the mutant liver.

Shp2 deficiency down-regulates central proliferative signals and MET expression

The results described above suggest ironically that Shp2 loss in hepatocytes triggered a tumor-promoting microenvironment in the liver. Thus, the inhibitory effect of Shp2 loss on the oncogenes-driven tumorigenesis is likely attributed to suppression of cell-intrinsic oncogenic signaling. To address this issue, we interrogated the central proliferative signaling events in these two animal tumor models. Immunoblotting of liver lysates demonstrated that exogenous MET/CAT expression induced marked increase of p-Erk signals (Fig. 5A), while MET/PIK injection enhanced p-Akt levels (Fig. 5B). Shp2 loss suppressed MET/CAT-induced p-Erk and MET/PIK-induced p-Akt activation, as examined at different time points (Fig. 5A–B). However, the induction of these proliferative signals by MET/CAT or MET/PIK was not affected by Ikkβ deletion (Supplementary Fig. 3D–E), consistent with the similar tumorigenic phenotypes in *WT* and *Ikkβ*$^{hep-/-}$ livers (Supplementary Fig. 3A–B).

We then examined the exogenous expression of hMET, β-catenin and PIK3CA in the liver at different time points. hMET- or Δβ-catenin-positive colonies expanded progressively in *WT* livers, but these signals were detected in *Shp2*$^{hep-/-}$ livers only at day 7 and disappeared at week 5 and 8 (Fig. 5C). p-Erk signal was detected by immunostaining in *WT* but not in Shp2-deficient hepatocytes at week 5 and 8 (Fig. 5D). The p-Erk signal detected in mutant liver lysates (Fig. 5A) is likely from non-parenchymal cells, as observed in Fig. 5D. Similar differences in hMET expression were observed between *WT* and *Shp2*$^{hep-/-}$ livers at week 6, 9 and 12 after MET/PIK injection (Fig. 5E). At week 10, hMET-positive colonies formed in *WT* liver were also CD133-positive, which were not seen in *Shp2*$^{hep-/-}$ liver (Supplementary Fig. 5A). Reduced expression of c-MET was even detected at day 3 after plasmid injection (Supplementary Fig. 5B–C), suggesting that Shp2 deficiency resulted in downregulation of the upstream RTK, c-MET. Similarly, previous experiments demonstrated significantly reduced levels of c-Kit and PDGFRβ in Shp2-deficient hematopoietic cells and fibroblasts, respectively[26,27]. Therefore, the Shp2 function in promoting RTK signaling is at least in part contributed by its ability to sustain the upstream RTK expression or stability, with the underlying mechanism to be elucidated.

We also determined the impact of Shp2 loss on Wnt/β-catenin signaling, by examining p-β-catenin levels and expression of downstream target genes. Phosphorylation of endogenous β-catenin at Ser33/37/Thr41 was not affected by MET/CAT transfection in *WT* or *Shp2*$^{hep-/-}$ livers (Fig. 5A). However, glutamine synthetase (Gl Syn)-expressing hepatocytes expanded beyond the perivenous areas progressively in *WT* but not in *Shp2*$^{hep-/-}$ livers (Fig. 5D).

Shp2 modulates mitogenic signaling elicited by HGF and Wnt3a in the liver

We further investigated the impact of Shp2 removal on HGF and Wnt signaling following portal vein administration of the ligands into the liver. Injection of HGF potently stimulated p-Met, p-Erk and p-Akt signals, but these signals were abolished or diminished in *Shp2*$^{hep-/-}$ livers (Fig. 6A), confirming the requirement of Shp2 in mitotic signaling. Wnt3a plus R-spondin1 stimulation did not alter Ser/Thr phosphorylation of β-catenin, nor its nuclear translocation in *WT* or *Shp2*$^{hep-/-}$ livers (Supplementary Fig. 6). However, the ligand injection induced low level of p-Erk signal in *WT* liver, which was abolished by Shp2 loss (Fig. 6A). Consistently, treatment of isolated primary hepatocytes by HGF or Wnt3a *in vitro* induced higher p-Erk signal in *WT* than Shp2-deficient hepatocytes (Fig. 6B). qRT-PCR analysis also demonstrated variably impaired expression of Wnt target genes, such as *ccnd1, cldn1, fst, jun, myc, mitf* and *enpp2*, in Shp2-deficient hepatocytes following HGF and/or Wnt3a stimulation (Fig. 6C).

Shp2 removal promotes cell senescence induced by oncoproteins

We explored whether Shp2 deficiency in hepatocytes promoted cell senescence in response to transfection of the oncogenes. Staining of liver sections demonstrated significantly increased signals for the primary senescence marker SA-β-galactosidase (β-gal) in *Shp2*$^{hep-/-}$ livers, compared to *WT* livers, at 7 and 12 days after transfection of MET/CAT or MET/PIK, respectively (Fig. 7A, Supplementary Fig. S7). Consistently, qRT-PCR analysis detected higher expression of cell cycle inhibitors p16 and p19 in *Shp2*$^{hep-/-}$ than control liver lysates, in response to expression of the oncogenes (Fig. 7B). Meanwhile, dividing cell numbers were decreased in *Shp2*$^{hep-/-}$ livers compared to *WT* livers, as assessed by Ki67 and HNF4α staining (Fig. 7C). β-gal signals diminished in *Shp2*$^{hep-/-}$ liver at week-3, and were barely detectable at week-5 post-injection (Supplementary Fig. 7), suggesting clearance of cells undergoing senescence. Together, these results suggest that deleting Shp2 in hepatocytes not only inhibited proliferative signaling but also induced cell senescence, collectively contributing to the suppression of hepato-oncogenesis induced by MET/CAT or MET/PIK.

Discussion

The requirement of Shp2 in liver tumorigenesis driven by MET/CAT or MET/PIK identified in this study is in sharp contrast to the liver tumor-inhibitory role of Shp2 recently observed in the same *Shp2*$^{hep-/-}$ mouse line[6,7]. The paradoxical pro- and anti-oncogenic effects of Shp2 in HCC development are apparently associated with the nature of oncogenic signals, cellular context and microenvironment. Although removing Shp2 or Ikkβ similarly exacerbated DEN-induced HCC development[6,19], Ikkβ deficiency did not exhibit significant impact on hepatic tumorigenesis induced by these two pairs of oncogenes. We also found

that in contrast to the effect of Shp2 loss, β-catenin deficiency dramatically aggravated MET/CAT-driven HCC[28], although DEN-induced tumorigenesis was similarly enhanced in *Shp2*$^{hep-/-}$ and *ctnnb1*$^{hep-/-}$ livers[8].

The data reported here argue that Shp2, acting immediately downstream of RTKs, is indeed an indispensable promoter for RTK-driven liver tumorigenesis. Consistently, a most recent report indicated that inhibiting Shp2 by siRNA or chemical inhibitor suppressed proliferation of RTK-driven tumor cells in vitro but had no significant impact on growth of cancer cells that were transformed by further downstream signaling molecules[29]. One important mechanism for Shp2 acting positively downstream of c-Met is its ability to maintain stable expression of the upstream RTK. Similar to this observation, we have found in previous studies that PDGFRβ was downregulated in Shp2-deficient fibroblast cells[27], and c-Kit expression was suppressed in Shp2-deficient hematopoietic cells[30].

However, the mechanism of Shp2 activities in cell signaling is likely more complicated than its functional interplay with RTKs, which is evidenced by its multi-faceted roles in liver tumorigenesis. Shp2 loss led to downregulation of Ras-Erk signaling, a negative impact on cell proliferation and survival. However, deleting Shp2 enhanced Stat3 activity[6], and induced higher expression of IL-6 and other inflammatory cytokines in the hepatic stroma. Furthermore, Shp2 acts to coordinate FGF15/19 and bile acid signaling in control of bile acid biosynthesis[31]. Therefore, *Shp2*$^{hep-/-}$ mice manifested hepatic injuries, cholestasis, fibrosis, and inflammation, thereby creating a hepatic microenvironment conducive for liver tumorigenesis. Now, one unnerving question is why these chronic liver damages did not exacerbate tumorigenesis in *Shp2*$^{hep-/-}$ mice driven by MET/CAT or MET/PIK, which deliver potent oncogenic signals. A possible explanation is that suppression of intracellular RTK signaling by Shp2 deletion outweighed the tumor-promoting effect of the tumor-promoting microenvironment created in *Shp2*$^{hep-/-}$ liver. This proposal ensues that oncogenic activation of critical intracellular signaling pathways is the driving force, and the microenvironment provides conducive signals for liver tumorigenesis. Supporting this theory is the data that MET/CAT-driven HCC was indeed exacerbated in *ctnnb1*$^{hep-/-}$ liver, in which a tumor-promoting microenvironment was generated by β-catenin deficiency[28].

Since additional deletion of Shp2 enhanced hepatocarcinogenesis in *Pten*$^{hep-/-}$ livers[7], it is also hard to understand why Shp2 deletion suppressed MET/PIK-driven tumorigenesis. In theory, deletion of Pten or overexpression of PIK3CA should similarly promote the PI3K/Akt pathway. One possibility is that Shp2-promoted Ras-Erk signaling is stringently required for MET/PIK and MET/CAT-driven liver tumorigenesis. In particular, Shp2 is a critical player downstream of c-Met, a common partner for these two pairs of oncoproteins. The RNA-seq data suggest common and distinct mechanisms for liver tumorigenesis driven by MET/CAT and MET/PIK, respectively. Obviously, more work needs to be done to elucidate the disclosed pro- and anti-tumorigenic effects of Shp2 in the liver.

The fact that Shp2 is an essential mediator of oncogenesis driven by c-Met, β-catenin and PIK3CA allows us propose a molecular targeted therapy by pharmaceutical inhibition of this tyrosine phosphatase for HCC patients with dominant active mutations or over-expression of RTKs and other upstream molecules that require Shp2 in signal relay. However, inhibiting

Shp2 will inevitably generate a milieu of tumor-promoting molecular and cellular factors in the liver. These microenvironmental effectors produced secondary to inhibition of the primary oncogenic signals may be responsible for rapid tumor recurrence observed in the clinic. Simultaneous suppression of the primary and secondary tumorigenic signals may be a most effective means, to achieve lasting therapeutic benefits for liver cancer patients.

Supplementary Material

Refer to Web version on PubMed Central for supplementary material.

Acknowledgments

The authors wish to thank Dr. X Chen (UCSF) for generously providing the oncogene constructs and invaluable advice and suggestions to this study, Dr. N Varki (UCSD) for pathological examination of tumor samples, Drs. P Sun (Wake Forest) B. Dong (Baylor) for advice to cell senescence assay.

Financial Support Statement: This project was supported by NIHR01HL129763, R01CA176012 and R01CA188506 (to G.S.F.). K.K. was supported by a postdoctoral fellowship by Moores UCSD Cancer Center.

References

1. Ryerson AB, et al. Annual Report to the Nation on the Status of Cancer, 1975–2012, featuring the increasing incidence of liver cancer. Cancer. 2016; 122:1312–1337. [PubMed: 26959385]
2. Lai, LA., Zhao, C., Zhang, EE., Feng, GS. Protein phosphatases. In: Arino, J., Alexander, D., editors. Topics in Current Genetics. Vol. 5. Springer-Verlag; 2004. p. 275-299.
3. Neel BG, Gu H, Pao L. The ‘Shp’ing news: SH2 domain-containing tyrosine phosphatases in cell signaling. Trends Biochem Sci. 2003; 28:284–293. [PubMed: 12826400]
4. Chan RJ, Feng GS. PTPN11 is the first identified proto-oncogene that encodes a tyrosine phosphatase. Blood. 2007; 109:862–867. [PubMed: 17053061]
5. Tartaglia M, et al. Somatic PTPN11 mutations in childhood acute myeloid leukaemia. Br J Haematol. 2005; 129:333–339. [PubMed: 15842656]
6. Bard-Chapeau EA, et al. Ptpn11/Shp2 acts as a tumor suppressor in hepatocellular carcinogenesis. Cancer Cell. 2011; 19:629–639. [PubMed: 21575863]
7. Luo X, et al. Dual Shp2 and Pten Deficiencies Promote Non-alcoholic Steatohepatitis and Genesis of Liver Tumor-Initiating Cells. Cell Rep. 2016; 17:2979–2993. [PubMed: 27974211]
8. Feng GS. Conflicting roles of molecules in hepatocarcinogenesis: paradigm or paradox. Cancer Cell. 2012; 21:150–154. [PubMed: 22340589]
9. Lanaya H, et al. EGFR has a tumour-promoting role in liver macrophages during hepatocellular carcinoma formation. Nat Cell Biol. 2014; 16:972–981. 971–977. [PubMed: 25173978]
10. Wang Q, et al. Spontaneous Hepatocellular Carcinoma after the Combined Deletion of Akt Isoforms. Cancer Cell. 2016; 29:523–535. [PubMed: 26996309]
11. Tao J, et al. Modeling a human hepatocellular carcinoma subset in mice through coexpression of met and point-mutant beta-catenin. Hepatology. 2016; 64:1587–1605. [PubMed: 27097116]
12. Chen X, Calvisi DF. Hydrodynamic transfection for generation of novel mouse models for liver cancer research. Am J Pathol. 2014; 184:912–923. [PubMed: 24480331]
13. Shang N, et al. FAK is required for c-Met/beta-catenin-driven hepatocarcinogenesis. Hepatology. 2015; 61:214–226. [PubMed: 25163657]
14. Bard-Chapeau EA, et al. Concerted functions of Gab1 and Shp2 in liver regeneration and hepatoprotection. Mol Cell Biol. 2006; 26:4664–4674. [PubMed: 16738330]
15. Tward AD, et al. Distinct pathways of genomic progression to benign and malignant tumors of the liver. Proc Natl Acad Sci USA. 2007; 104:14771–14776. [PubMed: 17785413]
16. Thorpe LM, Yuzugullu H, Zhao JJ. PI3K in cancer: divergent roles of isoforms, modes of activation and therapeutic targeting. Nat Rev Cancer. 2015; 15:7–24. [PubMed: 25533673]

17. Wang C, et al. Activated mutant forms of PIK3CA cooperate with RasV12 or c-Met to induce liver tumour formation in mice via AKT2/mTORC1 cascade. Liver Int. 2016; 36:1176–1186. [PubMed: 26716908]
18. Wang EY, et al. Depletion of beta-catenin from mature hepatocytes of mice promotes expansion of hepatic progenitor cells and tumor development. Proc Natl Acad Sci USA. 2011; 108:18384–18389. [PubMed: 22042854]
19. Maeda S, Kamata H, Luo JL, Leffert H, Karin M. IKKbeta couples hepatocyte death to cytokine-driven compensatory proliferation that promotes chemical hepatocarcinogenesis. Cell. 2005; 121:977–990. [PubMed: 15989949]
20. He G, et al. Hepatocyte IKKbeta/NF-kappaB inhibits tumor promotion and progression by preventing oxidative stress-driven STAT3 activation. Cancer Cell. 2010; 17:286–297. [PubMed: 20227042]
21. Pikarsky E, et al. NF-kappaB functions as a tumour promoter in inflammation-associated cancer. Nature. 2004; 431:461–466. [PubMed: 15329734]
22. Zeller KI, Jegga AG, Aronow BJ, O'Donnell KA, Dang CV. An integrated database of genes responsive to the Myc oncogenic transcription factor: identification of direct genomic targets. Genome Biol. 2003; 4:R69. [PubMed: 14519204]
23. Boutros R, Lobjois V, Ducommun B. CDC25 phosphatases in cancer cells: key players? Good targets? Nature reviews. Cancer. 2007; 7:495–507. [PubMed: 17568790]
24. Junttila MR, Evan GI. p53–a Jack of all trades but master of none. Nature reviews Cancer. 2009; 9:821–829. [PubMed: 19776747]
25. Huen MS, Sy SM, Chen J. BRCA1 and its toolbox for the maintenance of genome integrity. Nat Rev Mol Cell Biol. 2010; 11:138–148. [PubMed: 20029420]
26. Zhu HH, et al. Kit-Shp2-Kit signaling acts to maintain a functional hematopoietic stem and progenitor cell pool. Blood. 2011; 117:5350–5361. [PubMed: 21450902]
27. Lu X, Qu CK, Shi ZQ, Feng GS. Downregulation of platelet-derived growth factor receptor-b in Shp-2 mutant fibroblast cell lines. Oncogene. 1998; 17:441–448. [PubMed: 9696037]
28. Liang Y, et al. Beta-Catenin Deficiency in Hepatocytes Aggravates Hepatocarcinogenesis Driven by Oncogenic beta-Catenin and MET. Hepatology. 2017
29. Chen YN, et al. Allosteric inhibition of SHP2 phosphatase inhibits cancers driven by receptor tyrosine kinases. Nature. 2016; 535:148–152. [PubMed: 27362227]
30. Zhu HH, et al. Shp2 and Pten have antagonistic roles in myeloproliferation but cooperate to promote erythropoiesis in mammals. Proc Natl Acad Sci USA. 2015; 112:13342–13347. [PubMed: 26460004]
31. Li S, et al. Cytoplasmic Tyrosine Phosphatase Shp2 Coordinates Hepatic Regulation of Bile Acid and FGF15/19 Signaling to Repress Bile Acid Synthesis. Cell Metab. 2014; 20:320–332. [PubMed: 24981838]

Highlights

- Mouse liver tumor was induced by hydrodynamic transfection of 2 oncogenes.
- Shp2 loss suppresses liver tumorigenesis driven by MET/β-catenin or MET/PIK3CA.
- Shp2 deficiency triggers a tumor-promoting hepatic microenvironment.
- An effective therapy must block both cell-intrinsic and stromal oncogenic signals.

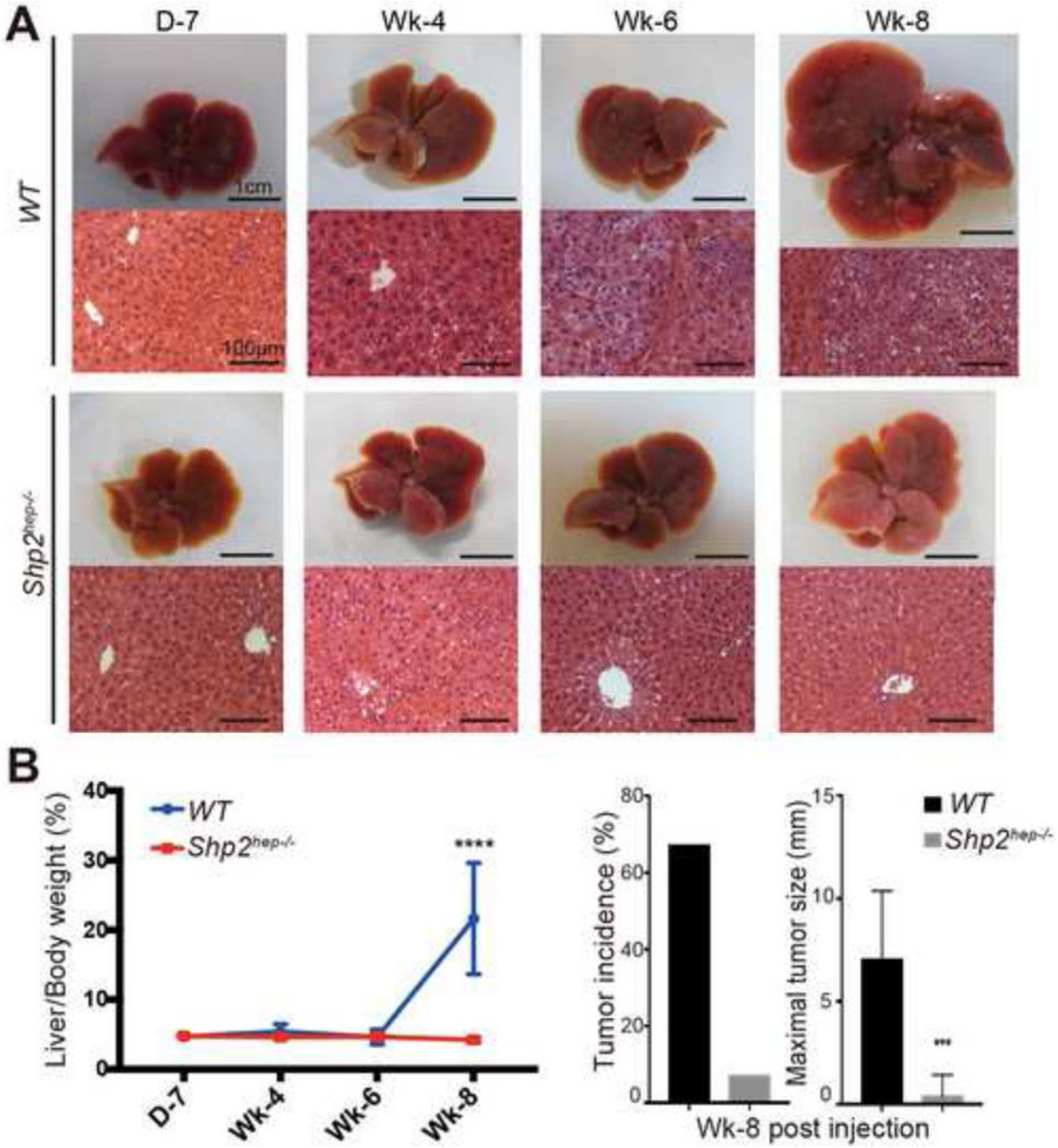

Fig. 1. Shp2 deletion suppresses MET/CAT-induced hepatocellular cancer

(A). Macroscopic images and H&E staining of mouse liver sections at day 7 and week 4, 6 and 8 post-hydrodynamic injection of *hMET* and Δ*β-Catenin* (MET/CAT) constructs. Scale bars: 1 cm (macroscopic); 100 μm (microscopic).

(B). Liver versus body weight ratios were measured at various time points (n=3, day-7; week 4 and week 6; n=8, week 8). Tumor incidences and maximal tumor sizes (n=8) were measured for *WT* and $Shp2^{hep-/-}$ mice at week 8 post-injection, and compared using student's t test. ***P<0.001, ****P<0.0001.

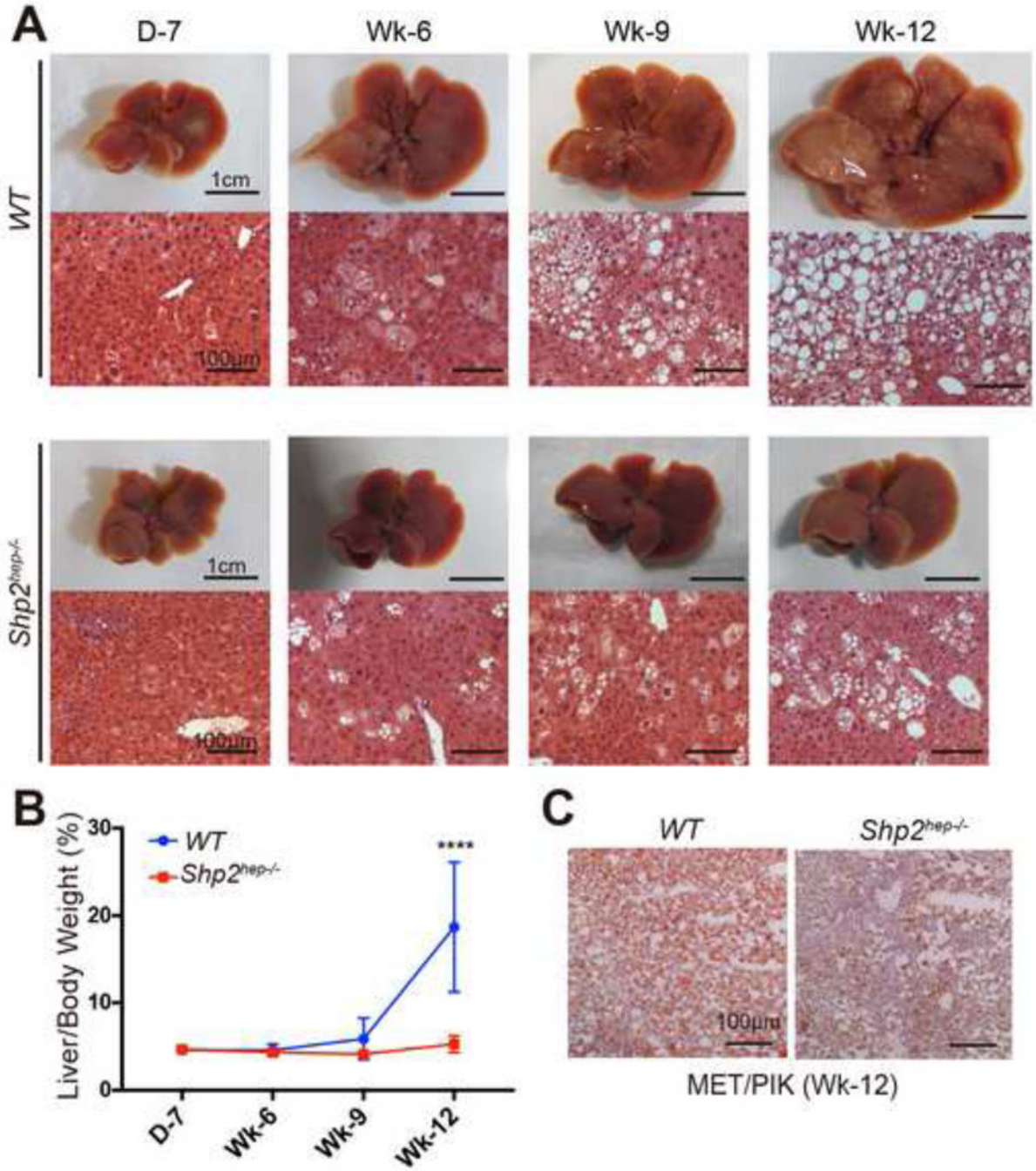

Fig. 2. Shp2 loss inhibits MET/PIK3CA-induced liver tumorigenesis

(A). Representative macroscopic images and H&E staining of mouse liver sections at various time points post injection of *hMET* and *PIK3CA* (MET/PIK) constructs. Scale bars: 1 cm (macroscopic), 100 μm (microscopic).

(B). Liver versus body weight ratios of MET/PIK-transfected mice were measure at various time points (n=3, D-7; n=4, Wk-6; n=4, Wk-9; n=7, Wk-12) (**** P<0.0001 by t test).

(C). Oil-Red-O staining of liver sections at week 12 post-injection of MET/PIK. Scale bars: 100 μm.

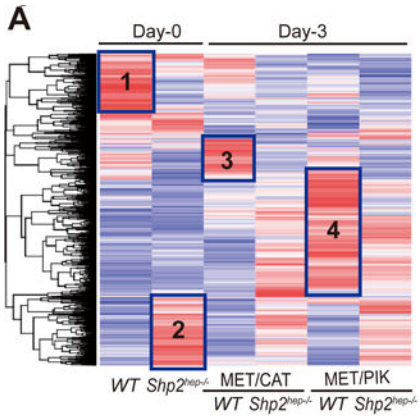

B

Highly enriched gene sets in cluster by GSEA	*P* value
Cluster 1: D-0 *WT* liver	
REACTOME: mRNA splicing	1.61E-07
KEGG: Spliceosome	3.28E-07
REACTOME: Processing of capped intron-containing pre-mRNA	5.12E-07
Cluster 2: D-0 *Shp2*$^{hep-/-}$ liver	
REACTOME: Metabolism of lipids and lipoproteins	6.52E-18
REACTOME: Cholesterol biosynthesis	5.65E-10
KEGG: Steroid biosynthesis	6.63E-09
REACTOME: PPARa activates gene expression	2.70E-07
KEGG: PPAR signaling pathway	4.32E-07

Highly enriched gene sets in cluster by GSEA	*P* value
Cluster 3: Met/Cat D-3 *WT* liver	
KEGG: Complement and coagulation cascades	1.28E-07
Cluster 4: Met/PIK D-3 *WT* liver	
REACTOME: Cell cycle	1.17E-21
PID: Aurora B pathway	7.94E-18
PID: PLK1 pathway	7.60E-11
REACTOME: DNA replication	3.11E-16
KEGG: ECM receptor interaction	5.89E-15
REACTOME: Immune system	1.33E-12
REACTOME: Cyclin A/B1 associated events during G2/M transition	1.92E-12

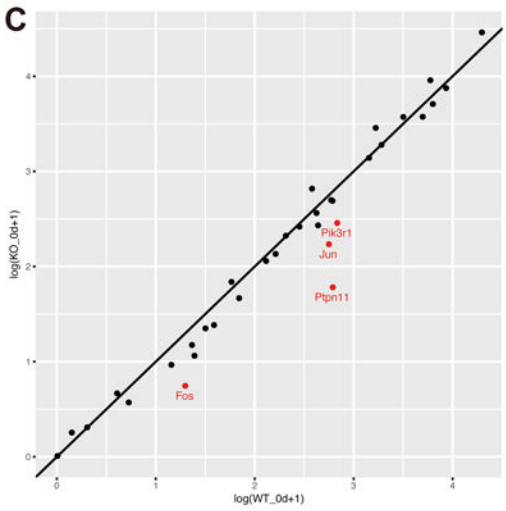

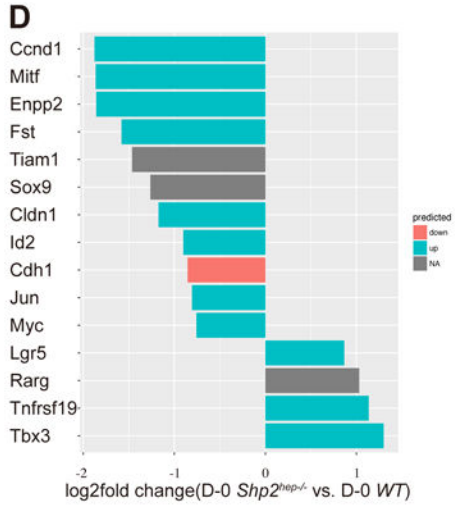

E

Pathways positively regulated by Shp2 deletion by IPA	*P* value
Glutathione-mediated Detoxification	1.26E-12
NRF2-mediated Oxidative Stress Response	2.57E-08
Superpathway of Cholesterol Biosynthesis	1.00E-06
Superpathway of Geranylgeranyldiphosphate Biosynthesis I (via Mevalonate)	1.00E-05
PXR/RXR Activation	5.89E-05
FXR/RXR Activation	1.10E-03
LXR/RXR Activation	0.011482

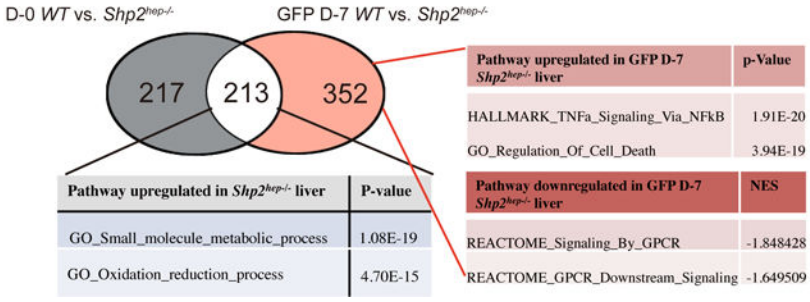

Pathway upregulated in *Shp2*$^{hep-/-}$ liver	P-value
GO_Small_molecule_metabolic_process	1.08E-19
GO_Oxidation_reduction_process	4.70E-15

Pathway upregulated in GFP D-7 *Shp2*$^{hep-/-}$ liver	p-Value
HALLMARK_TNFa_Signaling_Via_NFkB	1.91E-20
GO_Regulation_Of_Cell_Death	3.94E-19

Pathway downregulated in GFP D-7 *Shp2*$^{hep-/-}$ liver	NES
REACTOME_Signaling_By_GPCR	-1.848428
REACTOME_GPCR_Downstream_Signaling	-1.649509

Fig. 3. Comparative analysis of transcriptomes in *WT* and *Shp2*$^{hep-/-}$ livers

(A). Heatmap visualizing the FPKM values for differentially expressed genes across all 6 groups (n=3): *WT* and *Shp2*$^{hep-/-}$ livers before (Day-0) or after (Day-3) transfection of MET/CAT or MET/PIK, with red and blue indicating high and low gene expression, respectively. Highly expressed gene clusters are highlighted and numbered.

(B). GSEA analysis showing the most enriched gene sets in each highly expressed gene cluster.

(C). Comparison of baseline transcripts of HGF/c-Met targets between *WT* and *Shp2*$^{hep-/-}$ livers at Day 0. For each target gene, x- and y-axis values are its FPKM values in *WT* liver

and *Shp2*$^{hep-/-}$ livers, respectively. Printed in red are the genes expressed at significantly lower levels in *Shp2*$^{hep-/-}$ than *WT* livers.

(D). Comparison of transcript levels of Wnt target genes between *Shp2*$^{hep-/-}$ and *WT* livers at Day 0. Red, blue and grey colors indicate the genes down-regulated, up-regulated or not affected by the Wnt pathway.

(E). Ingenuity Pathway Analysis showing the top-ranked positively regulated pathways in *Shp2*$^{hep-/-}$ livers, relative to *WT* controls at Day 0.

(F). Overlap of differentially expressed genes (DEGs) in both Day-0 *WT* vs. *Shp2*$^{hep-/-}$ livers, and GFP Day-7 *WT* vs. *Shp2*$^{hep-/-}$ livers. The numbers indicate DEGs identified in both or only one comparison. Pathway analysis was performed on the DEGs from indicated groups.

A

Pathways positively regulated by Met/Cat on D-3 by IPA	*P* value
WT liver	
Hepatic Fibrosis / Hepatic Stellate Cell Activation	9.12E-06
Ubiquinol-10 biosynthesis	0.001696
DNA damage-induced 14-3-3σ Signaling	0.003467
Cell Cycle: G2/M DNA Damage Checkpoint Regulation	0.009550
Shp2$^{hep-/-}$ liver	
Agranulocyte Adhesion and Diapedesis	6.31E-12
Hepatic Fibrosis / Hepatic Stellate Cell Activation	1.23E-10
IL-10 Signaling	1.74E-05
Dendritic Cell Maturation	5.89E-05
GADD45 signaling	7.41E-05
p53 signaling	4.68E-04
Cell Cycle: G2/M DNA Damage Checkpoint Regulation	0.001995

B

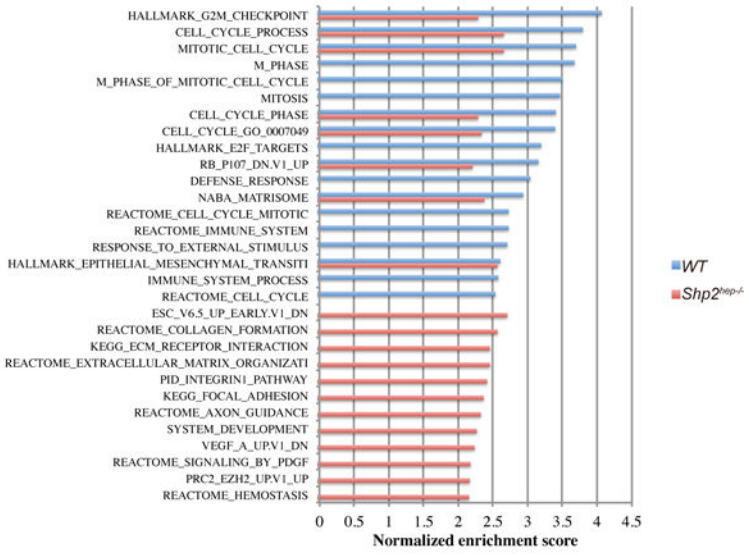

C

Pathways positively regulated by Met/PIK on D-3 by IPA	*P* value
WT liver	
Agranulocyte Adhesion and Diapedesis	3.16E-13
Granulocyte Adhesion and Diapedesis	5.01E-13
Hepatic Fibrosis / Hepatic Stellate Cell Activation	1.00E-11
Atherosclerosis Signaling	1.74E-08
Th1 and Th2 Activation Pathway	1.86E-07
Shp2$^{hep-/-}$ liver	
Hepatic Fibrosis / Hepatic Stellate Cell Activation	4.47E-10
Agranulocyte Adhesion and Diapedesis	9.77E-07
Mitotic Roles of Polo-Like Kinase	2.14E-06
GADD45 Signaling	4.17E-06
Cell Cycle: G2/M DNA Damage Checkpoint Regulation	7.94E-05
p53 Signaling	1.82E-04

D

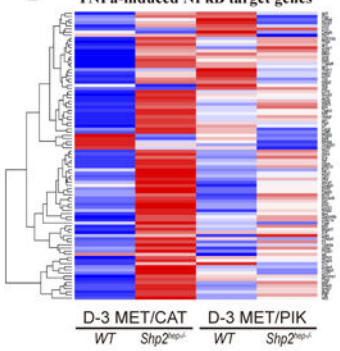

E

F

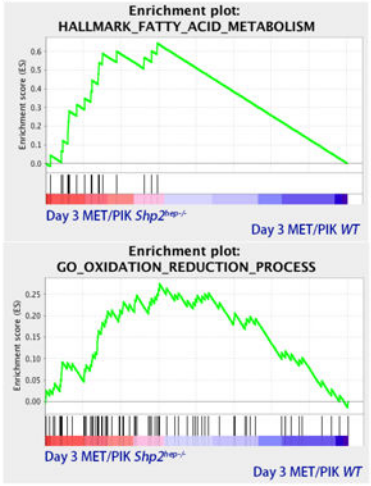

G

Pathway upregulated in MET/CAT D-7 *Shp2*$^{hep-/-}$ liver	NES
Defense_Response	2.8463962
REACTOME_Adaptive_Immune_System	1.9222717
MGGAAGTG_V$GABP_B	1.8392278

Pathway upregulated in MET/CAT D-7 *WT* liver	NES
Regulation_of_RNA_Metabolic_Process	-2.0009797
Regulation_of_Transcription_DNA_Dependent	-1.9949603
TGCCAAR_V$NF1_Q6	-1.9807506

H

Pathway upregulated in MET/PIK D-7 *WT* liver	NES
HALLMARK_G2M_Checkpoint	2.7814333
M_PHASE	2.5142448

Pathway upregulated in MET/PIK D-7 *Shp2*$^{hep-/-}$ liver	NES
REACTOME_Immune_System	1.804048
HALLMARK_Interferon_Gamma_Response	1.6097068

Pathway downregulated in MET/PIK D-7 *Shp2*$^{hep-/-}$ liver	NES
CACGTG_V$MYC_Q2	-2.5082772
GGGCGGR_V$SP1_Q6	-2.0140393

Fig. 4. Transcriptomic analysis of MET/CAT- or MET/PIK-transfected *WT* and *Shp2*$^{hep-/-}$ livers

(A)–(C). IPA of Day-3 MET/CAT-transfected *WT* or *Shp2*$^{hep-/-}$ livers versus Day-0 *WT* or *Shp2*$^{hep-/-}$ livers **(A)**; Top-ranked up-regulated gene sets in Day-3 MET/PIK-transfected *WT* or *Shp2*$^{hep-/-}$ livers versus Day-0 *WT* or *Shp2*$^{hep-/-}$ livers **(B)**; IPA of Day-3 MET/PIK-transfected *WT* or *Shp2*$^{hep-/-}$ livers versus Day-0 *WT* or *Shp2*$^{hep-/-}$ liver **(C).**

(D). Heatmap representation of TNFa-induced NF-kB target genes. Gene expression variations are presented by fold change of expression with red and blue indicating increase and decrease respectively, compared to genotype-matched Day-0 controls.

(E)–(F). Enrichment plots of gene set: CACGTG_V$MYC_Q2 comparing Day-3 MET/CAT-transfected *Shp2*$^{hep-/-}$ and *WT* livers **(E)**; gene sets: Hallmark_Fatty_Acid_Metabolism and Go_Oxidation_Reduction_Process comparing Day-3 MET/PIK-transfected *Shp2*$^{hep-/-}$ and *WT* livers **(F)**.

(G). GSEA analysis of DEGs between MET/CAT-transfected *Shp2*$^{hep-/-}$ and *WT* livers at Day 7.

(H). GSEA analysis of DEGs identified by comparing MET/PIK-*WT* livers versus GFP-*WT* liver at day 7, or MET/PIK-*Shp2*$^{hep-/-}$ livers versus GFP-*Shp2*$^{hep-/-}$ livers at day 7.

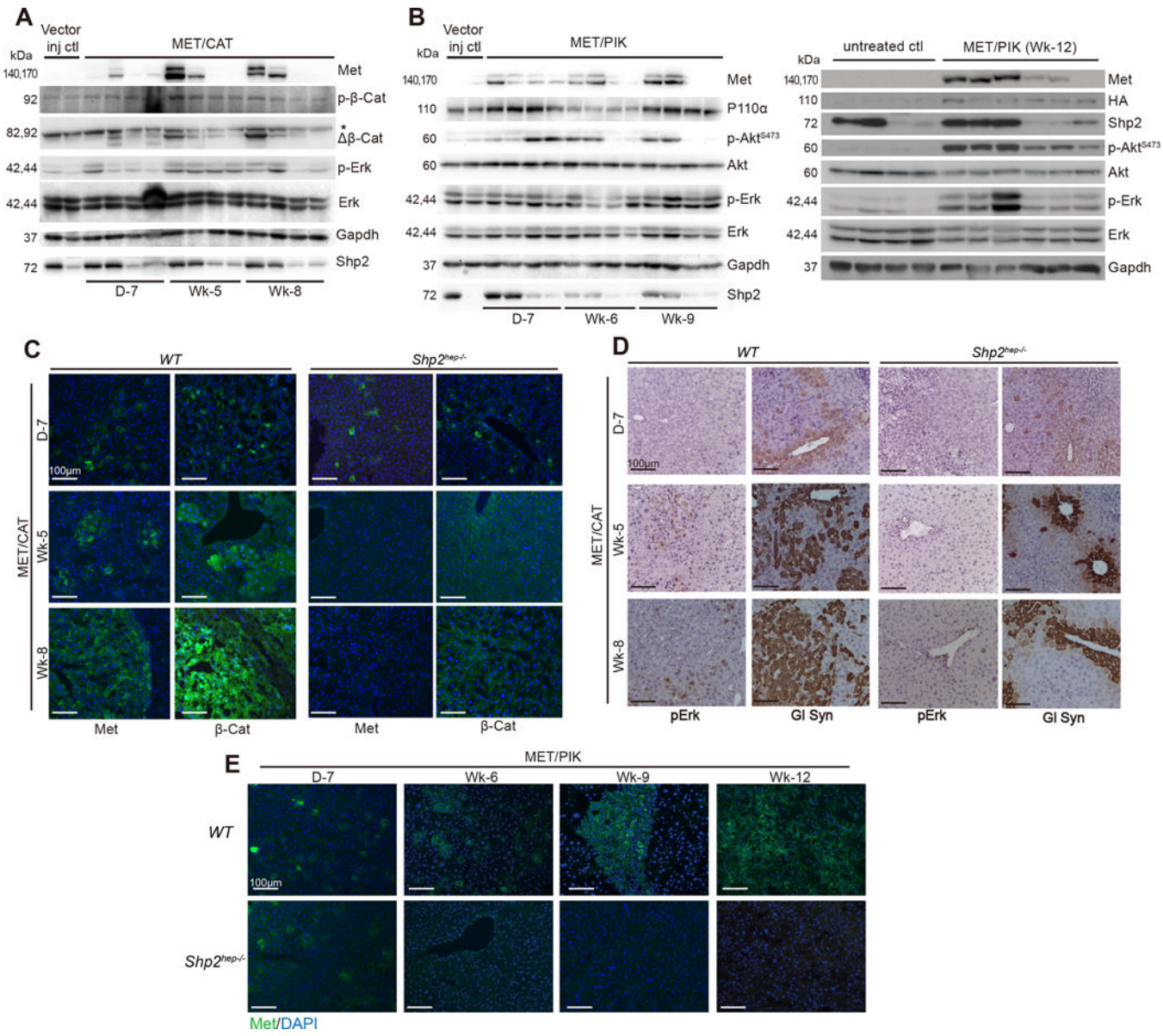

Fig. 5. Shp2 loss suppresses critical proliferative signaling events induced by the injected oncogenes

(A). Immunoblotting of liver lysates for the exogenous human c-Met and ΔN90-β-catenin (Δβ-cat), and p-Erk and Erk proteins at various time points after injection of MET/CAT, or a GFP vector control (* the endogenous β-catenin).

(B). Immunoblotting was performed for liver lysates collected at different time points after MET/PIK injection, to evaluate c-Met, p110α, and other signaling proteins as indicated, with a GFP vector control included.

(C). Immunostaining for exogenous c-Met and β-catenin on liver sections at day 7, week 5 and 8 post injection of MET/CAT. Scale bars: 100 μm.

(D). Immunostaining of glutamine synthetase (Gl syn) and p-Erk on liver sections prepared at day 7, week 5 and 8 post MET/CAT injection. Scale bars: 100 μm.

(E). Immunostaining of *WT* and *Shp2*$^{hep-/-}$ liver sections for exogenous c-Met at day 7, week 6, 9 and 12 post MET/PIK injection. Scale bars: 100 μm.

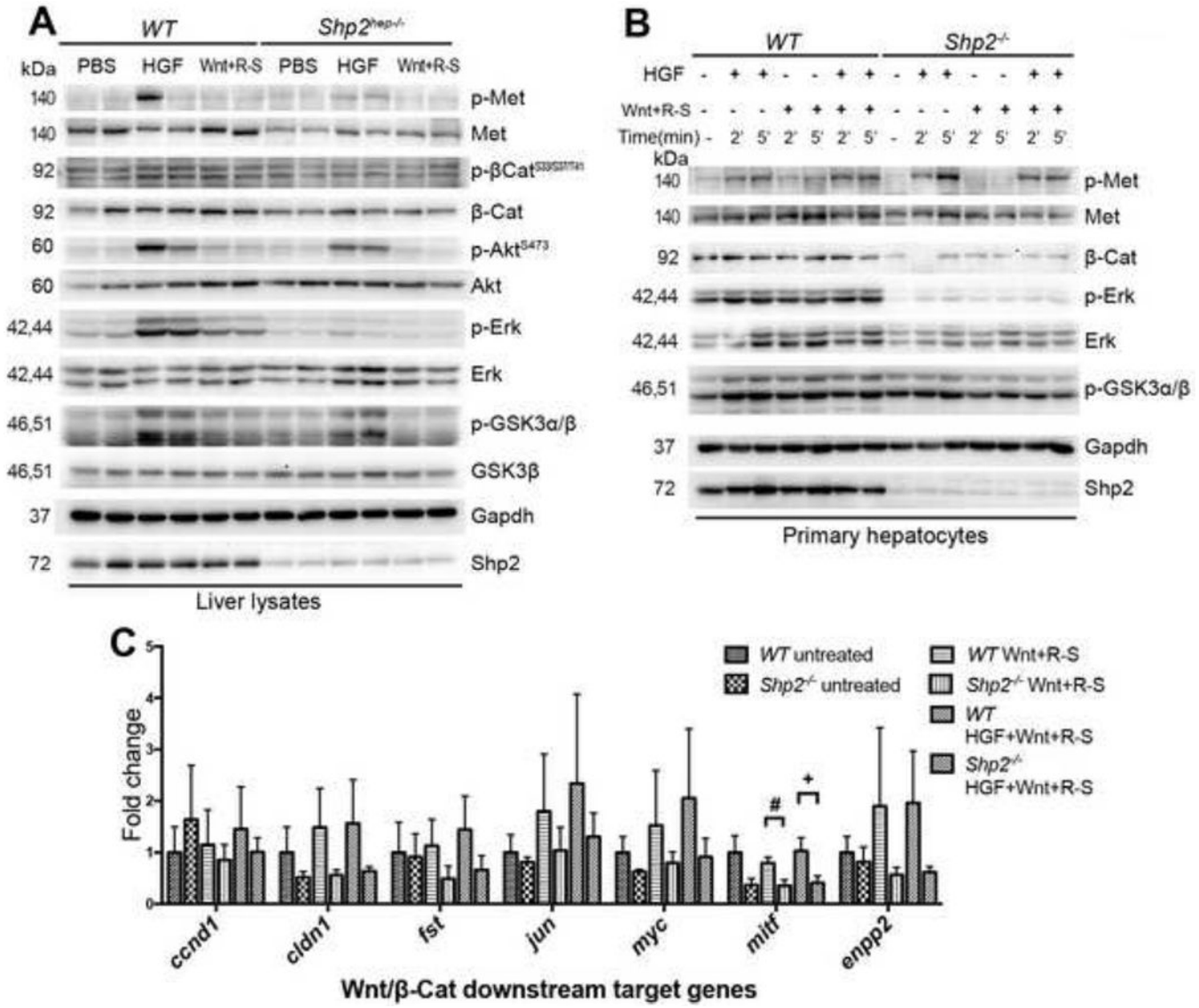

Fig. 6. Shp2 deficiency affects HGF and Wnt3a signaling *in vivo* and *in vitro*

(A). *WT* and *Shp2*$^{hep-/-}$ livers were stimulated through portal vein with HGF or Wnt3a plus R-Spondin1 *in vivo*. Immunoblotting of liver lysates was performed to examine phosphorylation of c-Met and β-Catenin and more downstream effectors, using antibodies as indicated.

(B). *WT* and *Shp2*$^{-/-}$ primary hepatocytes were isolated and then stimulated with HGF or Wnt3a plus R-Spondin1 for 2 or 5 minutes *in vitro*. Immunoblotting of cell lysates was performed to examine phosphorylated and total proteins of the components in HGF/c-Met and Wnt pathway, using indicated antibodies.

(C). qRT-PCR was performed to evaluate transcript levels of Wnt pathway target genes in *WT* and *Shp2*$^{-/-}$ primary hepatocytes stimulated with Wnt3a plus R-spondin1 (Wnt3a+R-S) or Wnt3a plus R-spondin1 and HGF (HGF+Wnt3a+R-S) for 1 hr (n=3, #P<0.05, +P<0.05 by t test)

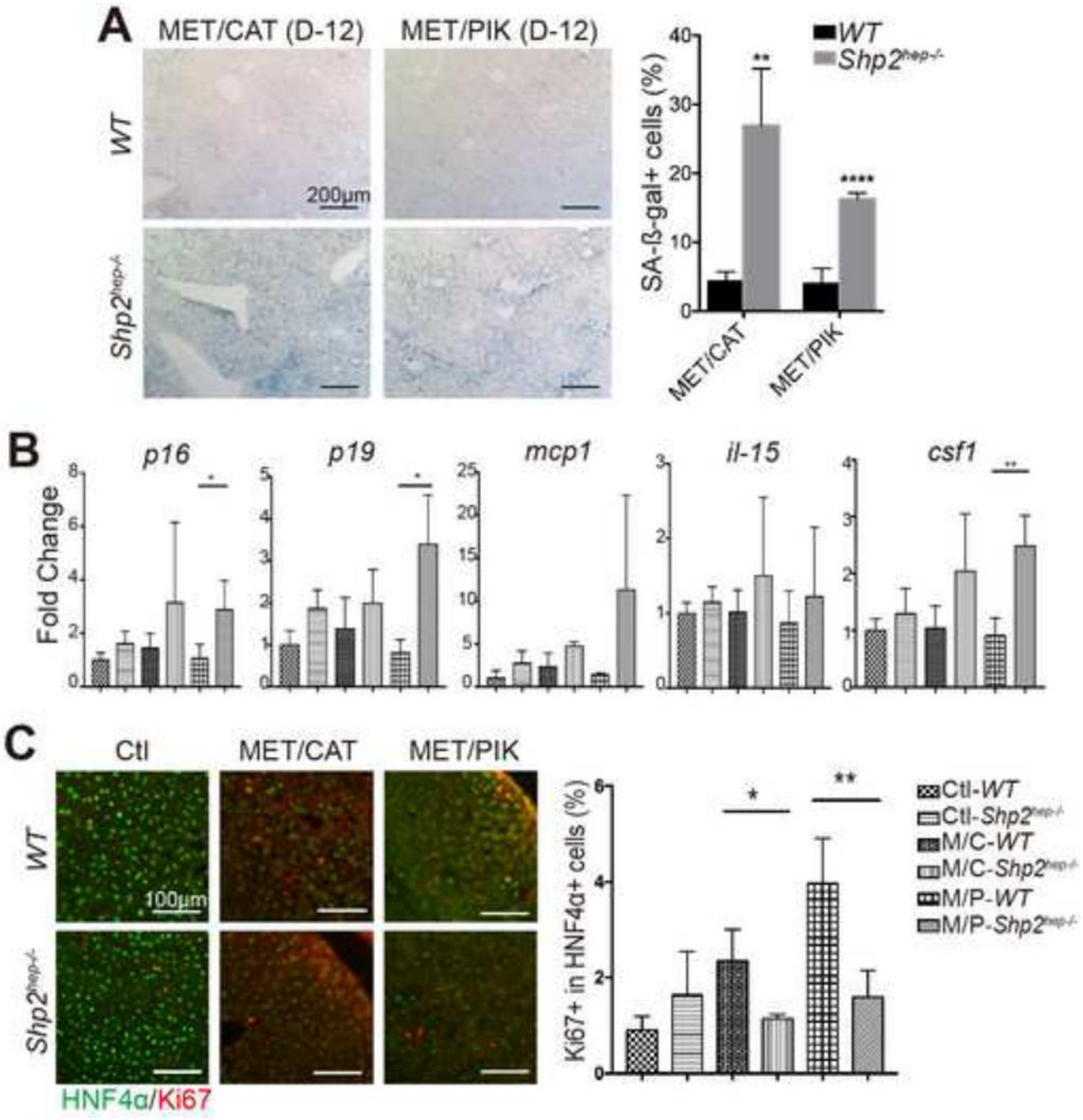

Fig. 7. Shp2 deficiency promotes oncogene-induced cell senescence

(A). Representative SA-β-galactosidase staining of *WT* and $Shp2^{hep-/-}$ liver sections at day12 after injection of MET/CAT or MET/PIK constructs. Percentage of SA-β-Gal-positive cells versus total cells is presented on the right as mean ± SE (n=3–4). Scale bars: 200 μm, ** $P<0.01$, **** $P<0.0001$ by t test.

(B). qRT-PCR was performed to determine relative expression of the genes as indicated (n=3–4). * $P<0.05$, ** $P<0.01$ by t test.

(C). Representative images of co-staining of HNF4α and Ki67 of liver sections on day 12 post injection. Percentage of $Ki67^+$ cells in total $HNF4\alpha^+$ cells was quantified and presented as mean ± SE (n=3–4). Scale bars: 100 μm, **P*<0.05, ***P*<0.01 by t test.